Meteorol. Z. (Contrib. Atm. Sci.), Vol. **28**, No. 3, 225–234 (published online April 1, 2019)

On the range of boundary layer model results depending on inaccurate input data

Günter Gross*

Institut für Meteorologie und Klimatologie, Universität Hannover, Germany

(Manuscript received November 8, 2018; in revised form February 12, 2019; accepted March 4, 2019)

Abstract

A one-dimensional boundary layer model was used to study the effects of uncertain input data on 2-m temperature and 10-m wind. Based on a very large number of numerical results, it can be demonstrated, that even a small degree of ambiguity can have significant implications, especially for temperature. In 50 % of all 6,000 simulations for flat terrain and randomly chosen sets of input data within narrow limits, temperature uncertainty was more than 2 K, and in 14 % of all cases more than 4 K, with a maximum of 9 K. Effect on wind speed is much smaller and depends mostly on surface roughness length. For a forest scenario, the results for temperature of 18,000 simulations are in the same order, with 25 % of the ensemble show temperature uncertainties of more than 2 K, and 6 % of more than 4 K, while wind speed above a forest is much more affected than for the bare soil case. In addition, the contribution of uncertainties of individual input data was estimated.

Keywords: boundary layer model, sensitivity study, input data uncertainties, flat terrain and forest

1 Introduction

Boundary-layer phenomena with typical length scales in the order of metres to kilometres and time scales between seconds and hours dominate and affect the appearance of the atmosphere near the ground. The main features of such phenomena are well-understood by the results of numerous observations in areas of different complexity, ranging from simple terrain (e.g. Dyer et al., 1971) to extremely heterogeneous environments like a city (e.g. Scherer et al., 2019). In addition, supplementary or alternative numerical models, which are suitable and specifically designed for the relevant scale, can be used (Früh et al., 2011; Gross, 2012; Hoffmann et al., 2018; Maronga et al., 2019).

Although these models deliver a wide variety of extremely helpful and valuable results, all models are always a simplification and imperfect abstraction of the real system, and thus involve inherent uncertainties. Such uncertainties largely result from incorrect model assumptions, different options for parameterisations and solution algorithms, or inadequate or erroneous information about input data. However, before apply any model, it will be carefully tested by developers and users with respect to numerical aspects (Jacob and Podzun, 1997; Ziemanski et al., 2011), model physics (Zhao et al., 2016; Demuzere et al., 2017) and input data (Liu et al., 2004; Diermeyer and Halder, 2016; Marzban et al., 2018).

Pertaining to the latter point, such a sensitivity analysis procedure explores and quantifies the impact of possible errors and uncertainties in input data on predicted outputs. In order to apply a numerical model, one must acknowledge that a large number of input data has to be specified, which may not be known with appropriate accuracy, and for lack of better information, published data from the literature are often adopted. However, although such data estimated from field experiments are representative of the specific site and the local conditions during the observations, they are hardly generalizable or transferable to other sites. Therefore, a specific input data is usually given in literature with a greater or lesser bandwidth. Model users decide to adopt a value out of this range that best agrees with their opinion or the most commonly used value.

A simple example demonstrates the possible consequences of selecting a specific value out of a set of uncertain data. Using a logarithmic wind profile to estimate the wind distribution in the lowest atmosphere near the ground, only friction velocity u_* and roughness length z_o represent necessary input data. For a fixed value of u_* ($u_* = 0.3$ m/s), a variation of z_o between 0.6 cm and 4 cm, which is representative for short grass (Etling, 2002), calculated wind speed at 10 m height differs by 1.4 m/s. However, roughness length especially is the input parameter, with a large number of published values for identical or similar land use, and so the user may be spoilt for choice (Hansen, 1993; Sozzi and Favaron, 1998; Pelletier and Field, 2016).

This example underlines the necessity of accurate input data, or, at least, based on a sensitivity study the expected range of the results for uncertain input information. The reaction of the model system to the simultaneous variation of a number of input data is even more complex as parameters of different uncertainty may interact in various ways.

*Corresponding author: Günter Gross, Institut für Meteorologie und Klimatologie, Universität Hannover, Herrenhäuser Str. 2, 30419 Hannover, Germany, e-mail: gross@muk.uni-hannover.de

DOI 10.1127/metz/2019/0952
Gebrüder Borntraeger Science Publishers, Stuttgart, www.borntraeger-cramer.com

In most published sensitivity studies, one parameter is changed and the resulting reaction of the model outputs is studied. In contrast, in this paper several parameters were changed simultaneously. However, in order to guarantee that nearly all possible combination options were captured and the entire parameter space was covered, several thousand numerical simulations with a simplified model were undertaken. This investigation was conducted for a flat terrain covered with low vegetation, and for a forest canopy with a higher stand.

2 The model

2.1 Model equations

Numerical simulations are restricted to horizontal homogeneous grassland and forests, and therefore model equations of a boundary layer model are simplified to a one-dimensional version with respect to the vertical z (Yamada, 1982; Gross, 1993). In order to limit the parameter space in this study, the effects of moisture and humidity are not considered in detail here. Model description is limited to the equations and parts of the model whereby the parameters considered here are included in the calculation. Further details may be found in Gross (1993) and Gross (2012).

$$\frac{\partial u}{\partial t} = f(v - v_g) + \frac{\partial}{\partial z} K_m \frac{\partial u}{\partial z} - \eta c_d b u|u| \tag{2.1}$$

$$\frac{\partial v}{\partial t} = -f(u - u_g) + \frac{\partial}{\partial z} K_m \frac{\partial v}{\partial z} - \eta c_d b v|v| \tag{2.2}$$

$$\frac{\partial \theta}{\partial t} = \frac{\partial}{\partial z} K_h \frac{\partial \theta}{\partial z} + \frac{1-\eta}{c_p \rho} \frac{\partial R}{\partial z} + \frac{\eta}{c_p \rho} \frac{\partial R_N}{\partial z} \tag{2.3}$$

$$\frac{\partial E}{\partial t} = \frac{\partial}{\partial z} K_m \frac{\partial E}{\partial z} + K_m \left[\left(\frac{\partial u}{\partial z} \right)^2 + \left(\frac{\partial v}{\partial z} \right)^2 \right] - K_h \frac{g}{\theta} \frac{\partial \theta}{\partial z} - \frac{E^{3/2}}{l} + \eta c_d b \left(|u|^3 + |v|^3 \right) \tag{2.4}$$

$$l_a = \frac{\kappa z}{1 + \kappa z / l_\infty}, \quad l_\infty = 25\,\text{m}, \quad \kappa = 0,40 \tag{2.5}$$

$$K_m = a l_a \sqrt{E}, \quad a = 0.2 \tag{2.6}$$

In the equations u and v are wind components in W–E and S–N direction, u_g and v_g components of the geostrophic wind, f Coriolis parameter, θ potential temperature, R is longwave radiation flux over unforested ground and R_N net radiation flux within the stand, E turbulence kinetic energy, l_a mixing length, K_m and K_h are eddy diffusivities for momentum and heat ($K_m = K_h$ is used here), g acceleration due to gravity, ρ air density, η fraction of an area covered with trees, c_d drag coefficient for a forest canopy and b leaf area density.

The effects of thermal stability on turbulent mixing in the boundary layer will considered by a stratification dependent mixing length

$$l = l_a / \Phi \tag{2.7}$$

Φ represents the local universal function which may according to Wippermann (1973) be expressed as

$$\Phi = (1 - 15z/L)^{-1/4}, \qquad z/L \le 0 \tag{2.8}$$
$$\Phi = 1 + 4.7z/L, \qquad z/L > 0$$

L denotes the Monin-Obukhov stability length.

The longwave radiation flux R from the sky above has been calculated for a given water vapour profile (Pielke, 2001) while at height h_t, the top of the canopy, R_N is given by

$$R_N(h_t) = (1 - a_t)S + R(h_t) - R_{L\Uparrow}(h_t) \tag{2.9}$$

The direct solar radiation S is estimated according to location and time and the outgoing longwave radiation is computed from (Yamada, 1982)

$$R_{L\Uparrow}(h_t) = \varepsilon_t \sigma T(h_t)^4 + (1 - \varepsilon_t) R(h_t) \tag{2.10}$$

a_t and ε_t are albedo and emissivity of the forest respectively. Vertical changes in the net radiation in the stand from the crown down to ground level are approximated by an exponential decrease:

$$R_N(z) = R_N(h_t) e^{-k\,\text{LAI}(z)} \tag{2.11}$$

k denotes an extinction coefficient and LAI leaf area index:

$$\text{LAI}(z) = \int_z^{h_t} b(z')dz' \tag{2.12}$$

The equations are solved on a staggered numerical grid (Arakawa C) and integrated forward in time. A grid interval of 2 m up to 30 m height and an expanded grid above up to 2,000 m is used.

2.2 Boundary conditions

At the upper boundary at a height of 2,000 m, an undisturbed situation is assumed with given values of wind ($u_g = 7$ m/s, $v_g = 0$ m/s), zero turbulence kinetic energy and a potential temperature of 297 K. The boundary conditions for wind at the ground are zero and turbulence kinetic energy E_o is proportional to local friction velocity squared

$$E_o = \frac{u_*^2}{a_o} = \frac{\kappa^2 u(z_1)^2}{a_o \left(\ln \frac{z_1}{z_o} - \Psi(z/L) \right)^2} \tag{2.13}$$

with the height z_1 of the first grid level in the atmosphere and a relation between Φ and Ψ as described by Stull (1988). For a_o, a value of $a_o = 0.4$ is used here.

Temperature at the ground T_o is determined by a surface energy budget that includes short-wave radiation:

$$Q_S = (1 - a) I_o \sin(h) \tag{2.14}$$

Table 1: Input data and range used in this study for flat terrain.

Input data	range	mean	equation	reference
z_o (m)	0.03–0.06 m	0.045	13	Etling, 2002
a	0.12–0.24	0.180	14	Pielke, 2001
λ (W/m/K)	0.7–1.0	0.85	16	Pielke, 2001, sand <10 % liquid water
Bo	day: 0.4 to 0.7	0.55	17	Stull, 1988
	night: −1 to −4	−2.5		
ε	0.95–0.98	0.955	15	Hupfer/Kuttler, 2006
T_{soil} (K)	290–293	291.5	16	

with albedo a, solar irradiance I_o and zenith angle h, outgoing long wave radiation

$$Q_L = \varepsilon\sigma T_o^4 \tag{2.15}$$

with emissivity ε and heat flux into the soil

$$Q_B = \lambda\frac{\partial T_S}{\partial z_S} \tag{2.16}$$

with λ thermal conductivity, T_S temperature in the soil and z_S depth in the soil. T_S will be calculated at nine levels inside the soil at depths of 2, 5, 10, 15, 20, 30, 50, 70 and 100 cm. It is assumed, that diurnal temperature variation is subsided at 1 m depth and here a constant value T_{soil} is adopted. Sensible heat flux Q_H is calculated by a flux-gradient relationship and latent heat flux Q_V is approximated by the Bowen ratio Bo:

$$Bo = Q_H/Q_V \tag{2.17}$$

This crude approximation is used here for simplicity and to restrict the number of input parameters that need to vary. Q_V is an essential part of the surface energy budget, but it depends on a wide range of additional and mostly unknown parameters such as soil moisture content or evaporation from trees.

3 Examination concept

Nearly all input data for the numerical simulations are accompanied by inherent uncertainties. Even small uncertainties may result in large differences in simulated outcomes. Here, the ensemble concept is adopted, where the results of a large number of simulations are used to estimate the quality and the uncertainties of the calculated distribution of meteorological variables in a statistical sense. Each member of the ensemble uses a slightly different configuration of a set of input data, albeit one falls within a realistic bandwidth.

For a flat terrain with low vegetation, selected surface characteristics are systematically modified according to the typical values listed in Table 1. The range is prescribed by small to moderate deviations around a characteristic mean found in the literature. The equation indicates, where a particular parameter enters the model.

Other ranges could of course have been chosen, but the intention of this study is to demonstrate the sensitivity of the results to moderate changes of uncertain input data.

Table 2: Input data and range used in this study for a forest canopy.

Input data	range	mean	equation	reference
h_t (m)	15–18	16,5	9	Giftthaler, 2017
η	0.6–0.9	0.75	1–4	
ε_t	0.93–0.96	0.945	10	Hupfer/Kuttler, 2006
a_t	0.17–0.20	0.185	9	Hupfer/Kuttler, 2006
c_d	0.1–0.4	0.25	1, 2, 4	Yamada, 1982, c_d = 0.2
k	0.5–0.8	0.65	11	Yamada, 1982, k = 0.6
f_b	0.9–1.1	1.0		

For the forest canopy case, the mean values of the parameters listed above are used, and only the modifications of forest characteristics are adopted (Table 2).

A typical deciduous canopy is used here with a flat-topped crown and the majority of the leaf mass found in the uppermost part of the crown with the amount decreasing rapidly downwards. As depicted in Fig. 1, this vertical distribution is modified by the factor f_b in order to consider the uncertainty in the vertical distribution of leafs. When varying the height of the stand, leaf area index LAI was fixed.

A large number of numerical simulations for different parameter combinations were performed each for a 10-day period in the summer in order to attain representative results with a nearly steady diurnal variation of the meteorological variables. The internal day-to-day variation for the final days of the period was less than 0.2 K for temperature and less than 0.02 m/s for wind speed. For the selection of the parameter values within the specified range, a random number generator providing uniform deviates between 0.0 and 1.0 was used. In order to guarantee the complete coverage of the parameter space, numerous simulations were required. To estimate this necessary number N, the range of each parameter is divided into three sections of equal length, e.g., z_o: 0.03–0.04 m, 0.04–0.05 m and 0.05–0.06 m. A complete coverage of the parameter space is given when all $n = 3^m$ elements (m = number of parameter) are filled at least with one combination. For six parameters, n is 729, and for seven parameters, n is 2,187. The total number N may be calculated by (Croucher, 2006)

$$N = nH_n. \tag{3.1}$$

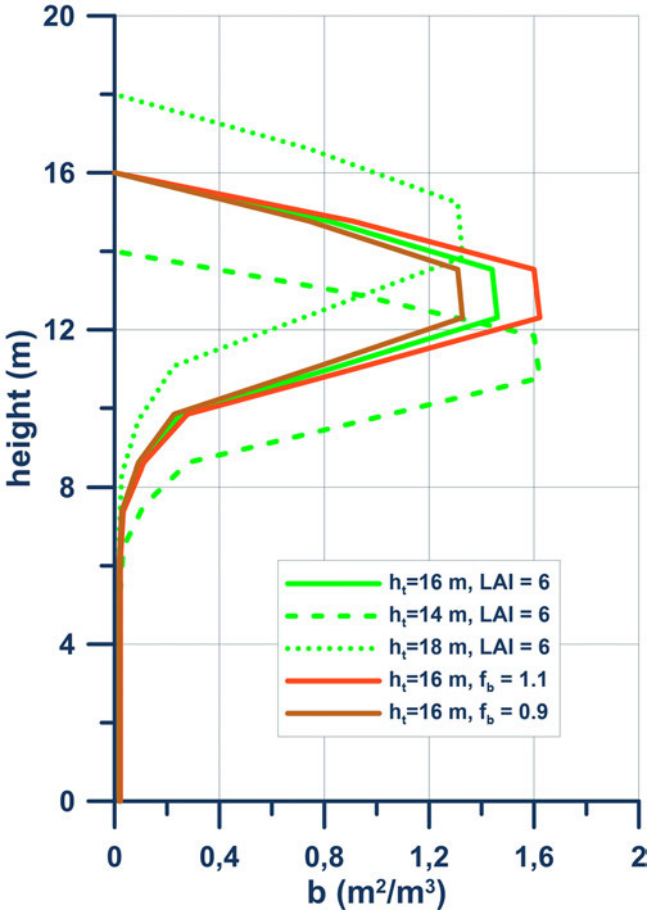

Figure 1: Vertical profiles of leaf area density.

with an approximation formula for the harmonic series H_n

$$H_n = \ln(n) + 0.5772 \tag{3.2}$$

For the approach adopted here with randomly chosen data, it follows, that for the flat terrain scenario, in which six input parameters are modified, a total number of more than 5,000 simulations are necessary to cover the complete parameter space, while this number increases for the forest scenario, with seven parameters at more than 18,000.

Evaluation of the calculations performed in this study demonstrates that such large numbers are necessary in order to capture, on average, all possible parameter combinations. The number of unfilled combinations in the parameter space decrease slowly with an increasing number of simulations, and only from 1,000 simulations is a strong decrease evident (Fig. 2). The final numbers (given in the lower right-hand corner of the figure) for the open field and the forest scenario are very comparable to the theoretically expected results.

4 Results

For each ensemble member with a slightly different set of input parameters, a ten-day summer simulation

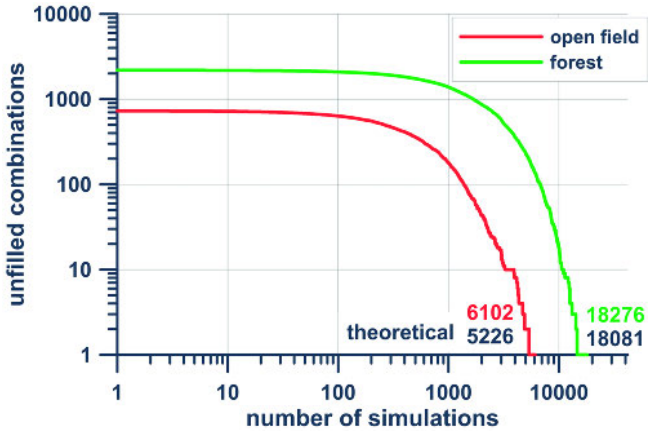

Figure 2: Number of unfilled parameter combinations with increasing number of simulations.

with constant synoptic forcing was performed, and the diurnal variation of the temperature and wind speed of the final day was used for evaluation. The focus in this study is the temperature at 2 m height and wind speed at 10 m height. However, for the forest canopy scenario, wind speed above the forest at a height of 20 m is used.

4.1 Results for flat terrain

The aim of this investigation was to study the complete combinations of the six parameters, hence more than 6,000 one-dimensional numerical simulations have been performed.

The typical and characteristic results for wind and potential temperature as a function of time and height are given in Fig. 3, for which the final day of the simulation period is displayed. During the day, a large amount of solar radiation warms up the ground, resulting in a near-neutrally stratified atmosphere up to a height of more than 1,000 m. In the afternoon hours, the energy budget becomes negative and the temperature decreases. This cooling of the ground continues into the night until the morning of the following day. During this period, an inversion forms, which is most pronounced around sunrise. Subsequently, the onset of solar radiation rapidly destroys this stable stratification. For this specific simulation, the temperature difference between night and day at a height of 2 m is in the order of 17 K. The variation of the temperature during the day and the associated modification of thermal stratification of the boundary layer also affects the mean wind significantly. During the day, enhanced turbulent mixing caused by the near surface unstably stratified atmosphere transports momentum from the layers above to the near surface region, resulting in high wind speeds. This transport is suppressed during stable stratification in the night-time hours, and the near surface wind is decoupled from the higher levels. Wind speed in this period near the surface is significantly lower than during the daytime. At a height of 100–200 m exists a shallow region with high wind speeds, known as the night-time low-level jet LLJ

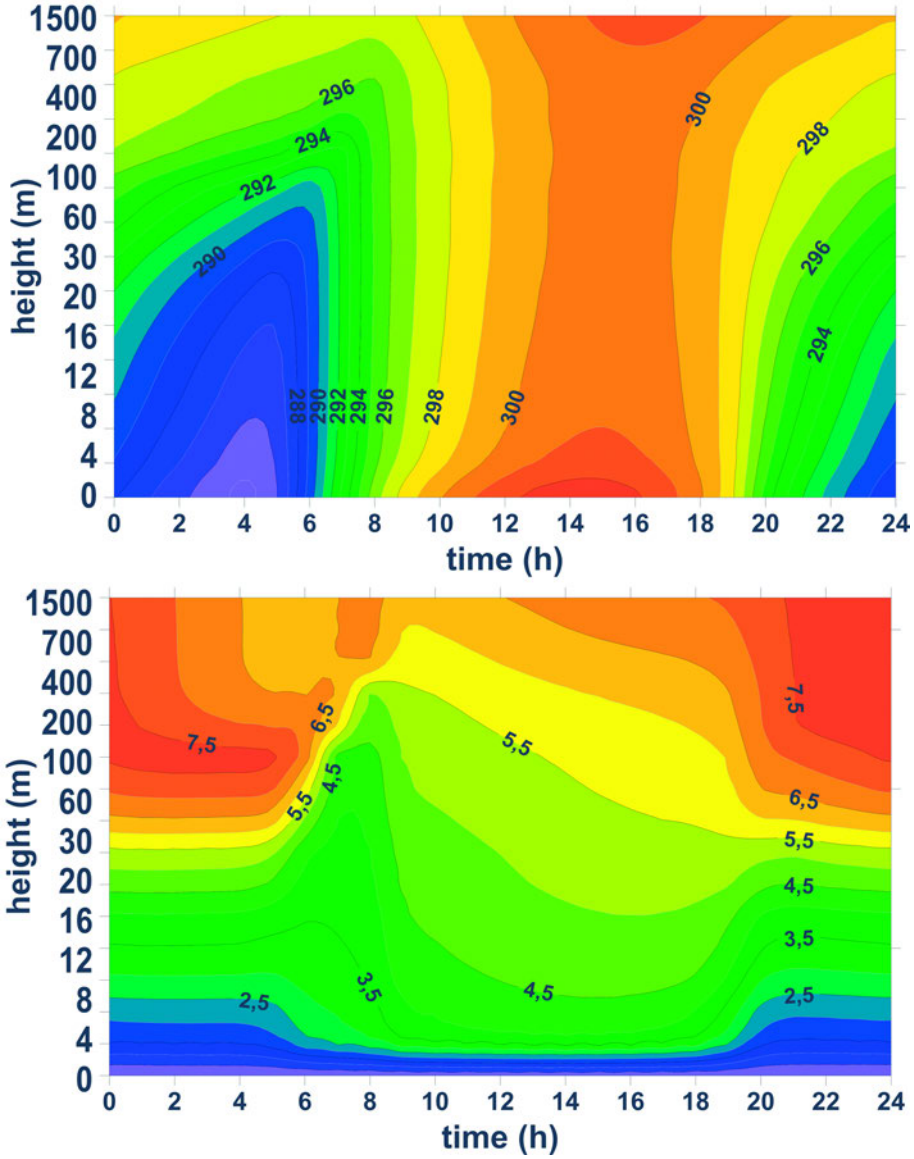

Figure 3: Exemplary result for flat terrain. Diurnal variation of potential temperature in K (top) and wind speed in m/s (bottom).

(Gross, 2012). This LLJ is especially prevalent in the second half of the night-time. After sunrise, the heating of the ground rapidly destroys the nocturnal inversion, while enhanced turbulent mixing ends the LLJ.

For each ensemble member, a ten-day simulation for a random combination of the parameters given in Table 1 was performed. All of the aforementioned parameters are of importance for the surface energy budget and surface temperature, and consequently for 2-m temperature as well. For the complete ensemble with more than 6,000, members night-time minimum temperatures and daytime maximum temperatures show a large bandwidth of values. Minimum temperature varies in the order of 10–16 °C and maximum temperature from 24 °C to 33 °C, with a nearly Gauss-shape of the frequency distribution (Fig. 4)

The diurnal variation of the differences within the ensemble are given in Fig. 5. For 2-m temperature the largest effect for different sets of input parameters is around 14 h with 8.8 K. A statistical evaluation results in a standard deviation of $\sigma = \pm 1.5$ K at the time of the temperature maximum around 14 h, and of $\sigma = \pm 1.1$ K before sunrise. In order to estimate the individual contribution of the selected parameter, 50 numerical simulations have been performed in which only one parameter was changed within the range given in Table 1, while for the remaining parameters the mean values are adopted. In order to minimise the uncertainty in temperature, surface roughness, albedo, thermal conductivity and Bowen-ratio all need to be available with very high accuracy. If these parameters are only known within the narrow bandwidth given in Table 1, a temperature uncertainty of around 3 K cannot be avoided. Emissivity and temperature in the soil are not insignificant, but have a smaller influence. Wind speed at 10 m height seems to be less sensitive than 2-m temperature and is largely affected by surface roughness. Maximum differences for all ensemble members are approximately 0.5 m/s

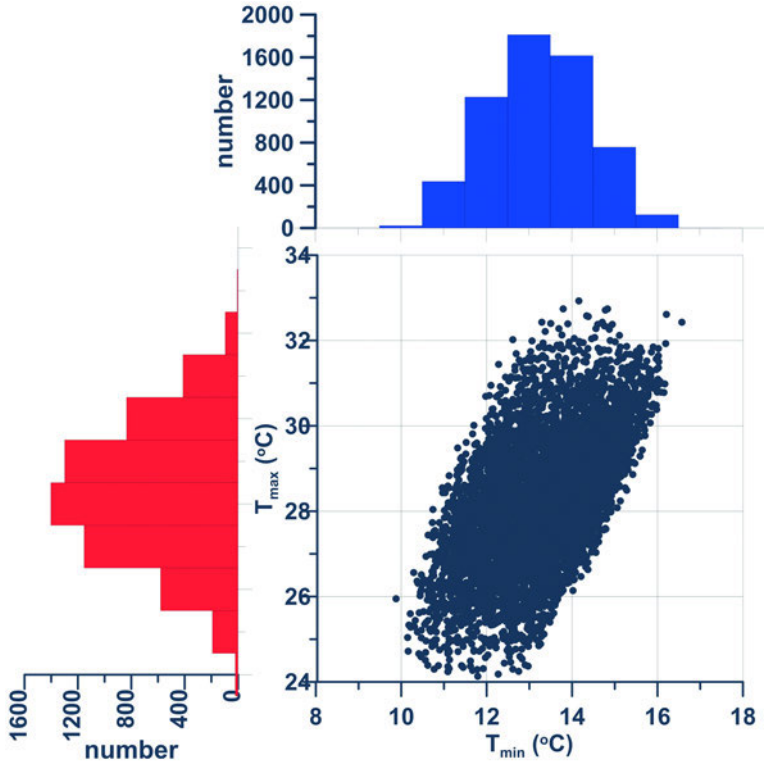

Figure 4: Scatter plot and frequency distribution of minimum (T_{min}) and maximum (T_{max}) 2-m temperature.

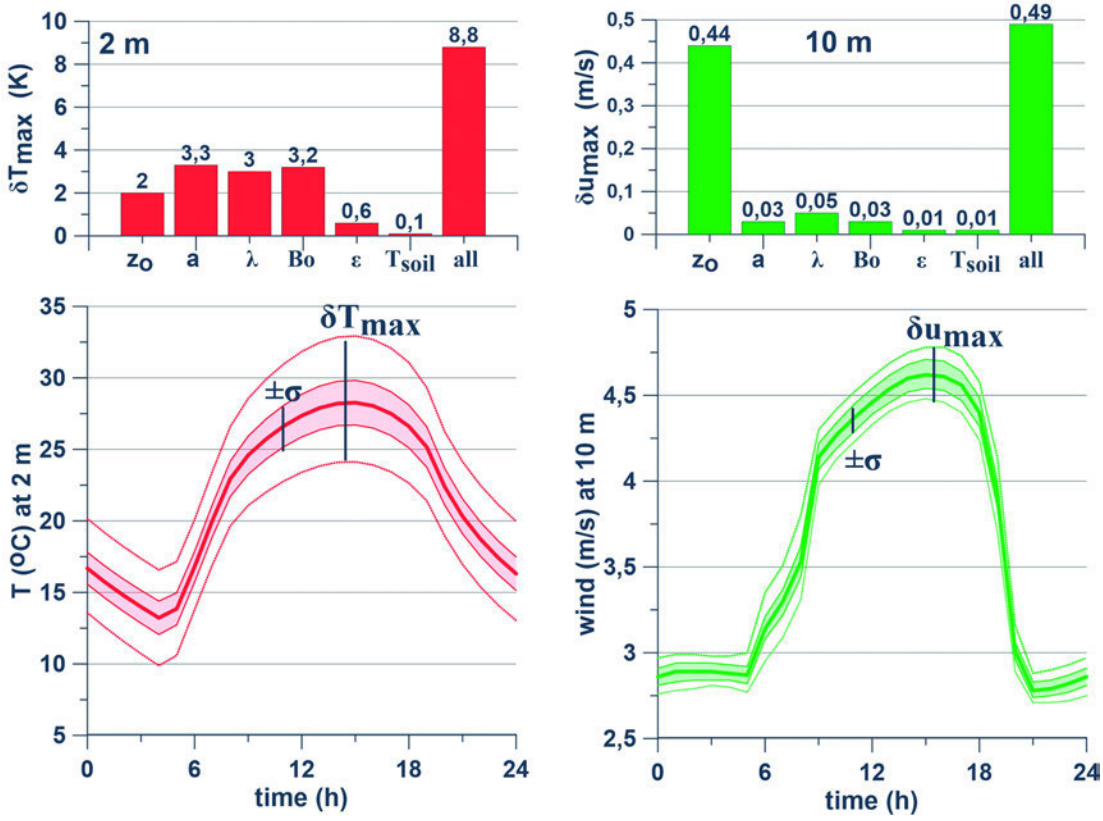

Figure 5: Below: Diurnal variation of maximum (δT_{max}) and mean differences (σ) within the ensemble for 2-m temperature and 10-m wind. Above: maximum differences for individual parameters only.

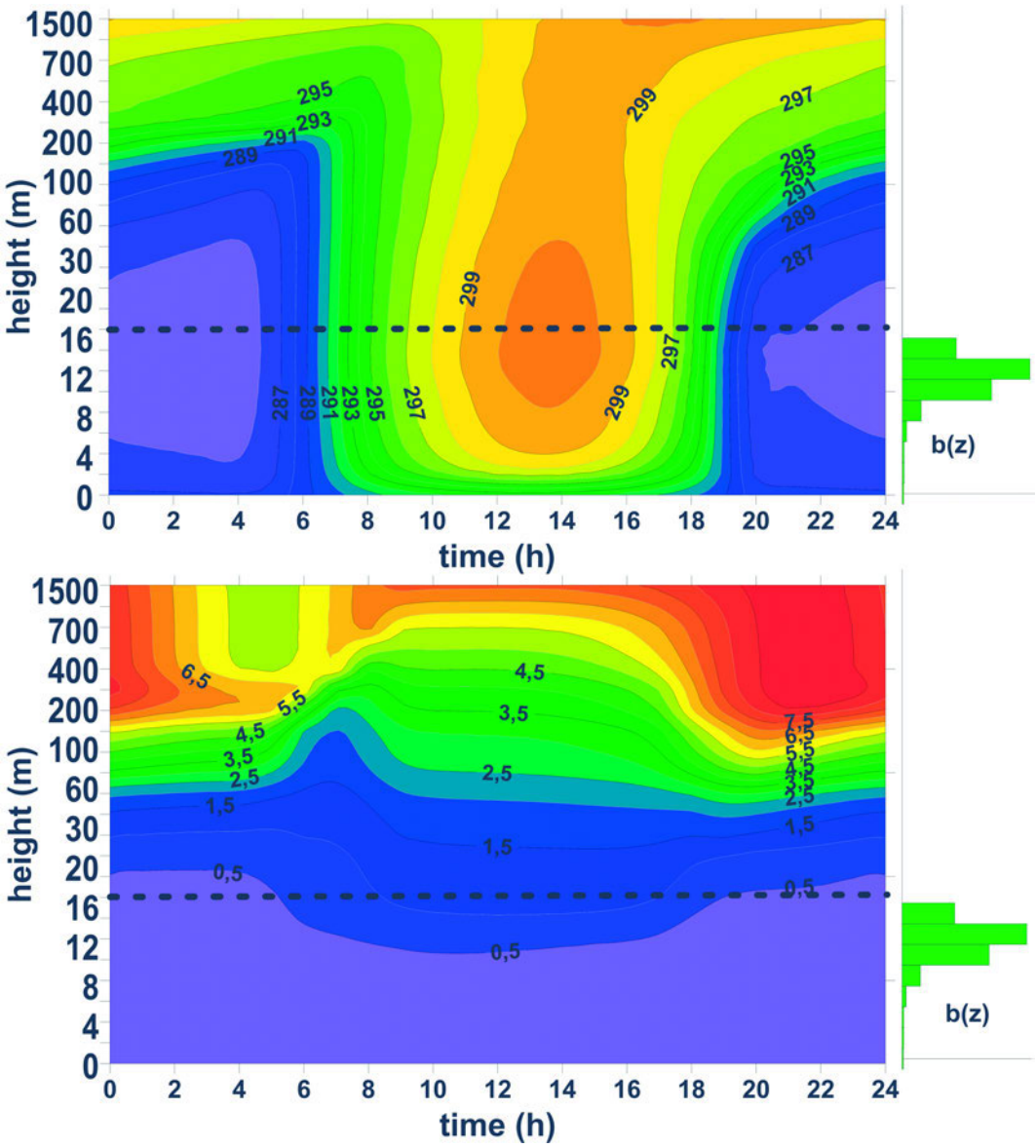

Figure 6: Exemplary result for a forest canopy. Diurnal variation of potential temperature in K (top) and wind speed in m/s (bottom). Vertical distribution of leaf area density is given on the right.

during the daytime for a mean wind at this time of around 4.5 m/s. The standard deviation is $\sigma = \pm 0.08$ m/s during the daytime and $\sigma = \pm 0.05$ m/s at night.

It should be pointed out, that the assumption of horizontal homogeneity (1D) underestimates horizontal and vertical mixing. If such processes are substantial they have the potential to reduce the very large temperature uncertainties. But there is also a risk, that simulated poor meteorological information from regions with imprecise input data will be advected in 3D to areas, where, in presence of very good input data, otherwise much better results would be calculated.

4.2 Results for a forest canopy

The evaluation has been extended to a more complex situation for a deciduous forest canopy. The effects of inaccurate seven input parameters, as given in Table 2, are studied. This results in more than 18,000 one-dimensional simulations in order to completely cover the parameter space. Again, the simulated characteristic features of wind and temperature as functions of time and height for a summer day are presented first (Fig. 6). The input parameters for this simulation are the mean values listed in Tables 1 and 2.

During the daytime, the dense canopy shields the ground from direct insolation. Direct solar radiation is mostly absorbed by the stand elements in the upper third of the canopy, resulting in an elevated temperature maximum within the crown. The location of this maximum depends strongly on the assumed vertical distribution of leaf area density and extinction coefficient k. During the night, the cooling of the air near the top of the canopy due to long-wave radiation is the reason for the elevated temperature minimum, with an unstably

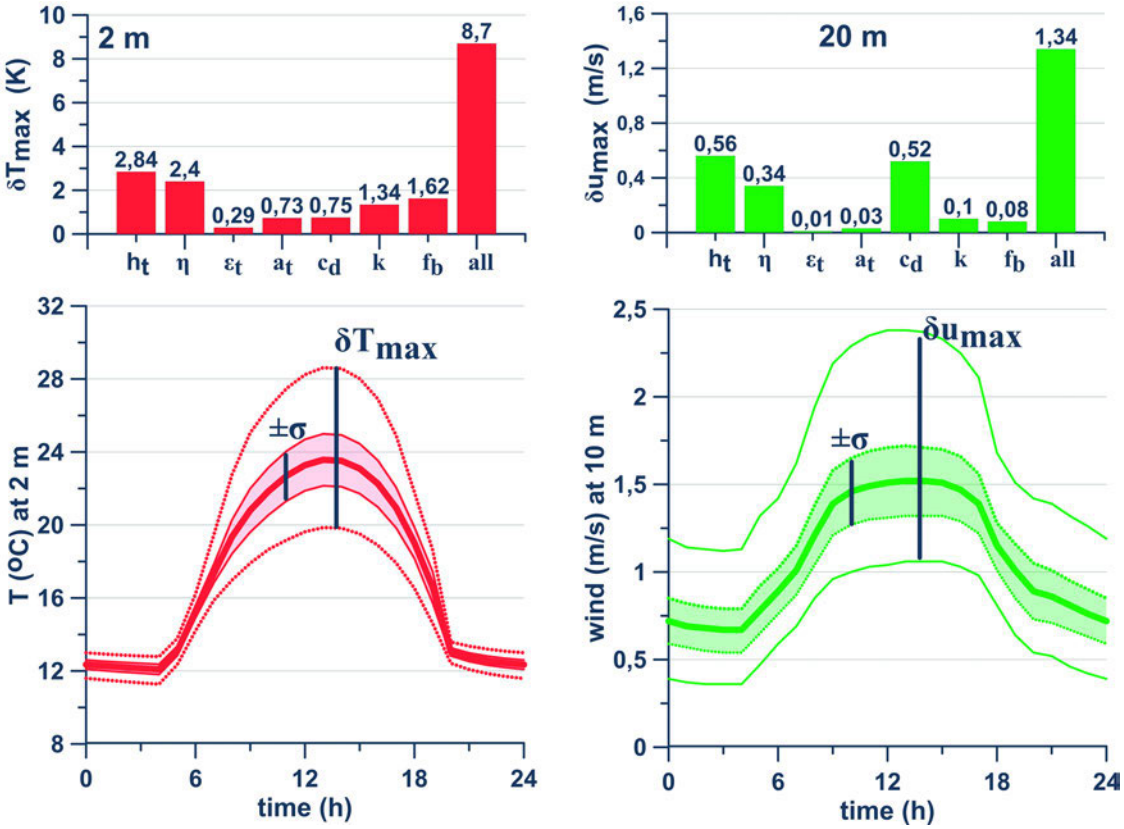

Figure 7: Below: Diurnal variation of maximum (δT_{max}) and mean differences (σ) within the forest ensemble for 2-m temperature and 20-m wind. Above: maximum differences for individual stand parameters only.

stratified atmosphere within the stand and an inversion above. Due to the protective properties of the crown, a diurnal variation of 2-m temperature is much smaller than for the bare soil case presented above. A prominent characteristic of the wind climate within the stand is a very low wind speed with small diurnal variations. Above this calm zone, a strong increase in wind speed is simulated with a well-developed low-level jet during the night-time at a height of 300–400 m. The location of this LLJ is higher and wind speeds are stronger than in the flat terrain case. Similar findings have been published by Yamada (1982) and Gross (1993).

The diurnal variations of the differences within the ensemble, consisting of 18,000 members, are given in Fig. 7. The largest 2-m temperature effect around 14 h is 8.7 K. The statistical analysis results in a standard deviation during the day of $\sigma = \pm 1.4$ K and of $\sigma = \pm 0.3$ K around the time of the temperature minimum during the night. Again, in order to estimate the individual contribution of the selected parameter, 50 numerical simulations have been performed, whereby only one parameter was changed within the range given in Table 2. For temperature, an inaccurate value of tree height and stand density may result in an error of 2.4–2.8 K, of k and f_b of around 1.5 K and of albedo and drag coefficient of 0.7 K. Only the emissivity of the tree is of minor importance. The evaluation for wind speed is not at a height of 10 m, which is inside the crown of the canopy, but well above the treetop at a height of 20 m. The height of the trees, stand density and drag coefficient largely determine the wind uncertainty and represent the most important parameters. The maximum difference for all ensemble members is approximately 1.3 m/s during the daytime for a mean wind at this time of around 1.5 m/s. The standard deviation is $\sigma = \pm 0.20$ m/s during the day and $\sigma = \pm 0.13$ m/s at night.

4.3 Probability of uncertainty

The easiest means of acquiring information regarding the probability of specific uncertainties from the ensemble is by simply counting the occurrence of certain results of the ensemble members. Such frequency distributions for wind and temperature are given in Fig. 8. For instance, a temperature uncertainty of 4 K implies a range of ±2 K. Small modifications in the parameters given in Table 1 and 2 may cause uncertainties in temperature in various magnitudes of up to nearly 9 K. For the open field case, the specified or expected accuracy of e.g. 2 K is given only in 50 % of the results of the ensemble and for 86 % of the ensemble members temperature uncertainties are smaller than 4 K. Inside the forest canopy with the damped diurnal variation the corresponding values are 75 % and 94 %. For wind speed the uncertainties caused by inaccurate input parameters are not as significant as for temperature, and in more than 95 % of the ensemble are usually smaller than 0.4 m/s for the open field and below 0.6 m/s above the forest.

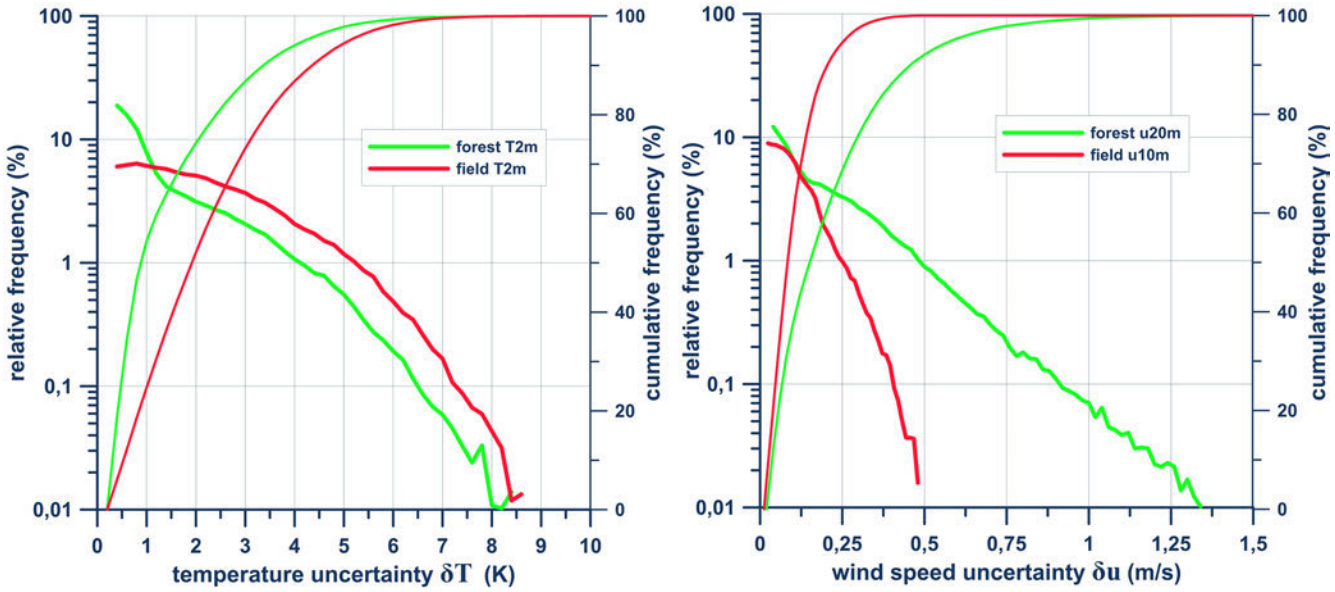

Figure 8: Relative and cumulative frequency distribution of temperature (left) and wind speed uncertainty (right) for an open field and a forest canopy.

5 Conclusions

A simple one-dimensional boundary layer model was used to study the effects of inaccurate input data on the simulated 2-m temperature and 10-m (20-m) wind. Two different land-use scenarios have been adopted for which different sets of input data must be prescribed. For the flat terrain with grass, the focus is on the variation of surface and soil parameter, while forest characteristics are modified for the scenario with high vegetation. Input data have been varied randomly within described limits, and for further evaluation they are divided into three discrete segments (nominal, high and low). Via a large number of numerical simulations it is guaranteed that the complete parameter space with all possible combinations of the input data is covered.

Statistical evaluation of a large number of calculated information (here: more than 6000) clearly highlights that even slightly inaccurate input data may cause substantial differences in the results. Although the variation of the input data for the flat terrain was narrow, in 50 % of the results the maximum temperature difference within a diurnal course was larger than 2 K, and in 14 % of the ensemble the temperature difference was larger than 4 K, with a maximum of around 9 K. The results permit the conclusion that all parameters considered here significantly contribute to temperature uncertainty. Only the emissivity of the ground and initial soil temperature are of minor importance. The effects on 10-m wind speed is less pronounced and dominated by the surface roughness length.

Beneath the forest canopy, the diurnal temperature variation and the effects of input data modification are smaller relative to the open field. For 25 % of the ensemble of 18,000 members the temperature effect is larger than 2 K, and in only 6 % of the cases the uncertainty is above 4 K. None of the seven selected parameters considered here is unimportant, with each contributing to some extent to the temperature uncertainty. Wind speed above the canopy is more significantly affected than the 10-m wind above grass, and it turns out, that tree height, stand density and the specification of a drag coefficient are of particular importance.

Only a certain selection of input data has been varied in this study. Depending on the specific subroutine and scheme used to calculate surface temperature, it is possible that many more parameters need to be prescribed. This is especially the case when soil moisture and evaporation from the vegetation are introduced into the model. These factors have not been considered in this study for purpose of simplicity. But if these processes are considered in the model in detail, a wealth of new input data with specific uncertainties are necessary.

The main finding of this study is the large range in simulated results of up to several degrees if the input data contain a small to moderate degree of inherent uncertainty. The results presented here are rough estimates which indicate the magnitude of the possible uncertainties and are no hard physical limits for temperature and wind forecast since a number of other factors like 3D instead of 1D or other input data, not considered here, may have significant effects as well. It is important to acknowledge that a comparison and verification of a model with observations can only succeed if the complete set of input data is available with extreme precision.

The user of a model is always confronted with the fact of more or less inaccurate input data. Here an ensemble prediction with different sets of data, covering the bandwidth of the uncertainties, can be recommended. However, for practical use of a mesoscale or microscale model, such an approach is usually limited by the resources available.

Acknowledgements

This paper is part of the MOSAIK-project, which is funded by the German Federal Ministry of Education and Research (BMBF) under Grant 01LP1601 within the framework of Research for Sustainable Development (FONA; www.fona.de).

References

Croucher, J.S., 2006: Collecting coupons – A mathematical approach. – Australian Senior Mathematics J. **20**, 31–35.

Demuzere, M., S. Harshan, L. Järvi, M. Roth, C.S.B. Grimmond, V. Masson, K.W. Oleson, E. Velasco, H. Wouters, 2017: Impact of urban canopy models and external parameters on modelled urban energy balance in a tropical city. – Quart. J. Roy. Meteor. Soc. **143**, 1581–1596.

Diermeyer, P.A., S. Halder, 2016: Sensitivity of numerical weather forecasts to initial soil moisture variations in CFSv2. – Wea. Forecast. **31**,1973–1983.

Dyer, A.J., R.R. Brook, D.G. Reid, A.J. Troup, 1971: The Wangara experiment: Boundary layer data. – Techn. Paper **19**, Div. Meteor. Phys CSIRO, Australia.

Etling, D., 2002: Theoretische Meteorologie. – Springer Verlag Heidelberg, 354 pp.

Früh, B., P. Becker, T. Deutschländer, J.-D. Hessel, M. Kossmann, I. Mieskes, J. Namyslo, M. Roos, U. Sievers, T. Steigerwald, H. Turau, U. Wienert, 2011: Estimation of climate-change impacts on the urban heat load using an urban climate model and regional climate projections. – J. Appl. Meteor. **50**, 167–180.

Giftthaler, M., 2017: Ermittlung von Einzelbaumhöhen basierend auf Fernerkundungsdaten unbemannter Luftfahrtsysteme. – J. Angewandte Geoinformatik **3**, 142–152.

Gross, G., 1993: Numerical simulation of canopy flows. – Springer Verlag Heidelberg, 167 pp.

Gross, G., 2012: Effects of different vegetation on temperature in an urban building environment. Micro-scale numerical experiments. – Meteorol. Z. **21**, 399–412.

Hansen, F.V., 1993: Surface roughness lengths. – Army Research Laboratory ARL-TR-61, White Sands NM.

Hoffmann, P., R. Schoetter, K.H. Schlünzen, 2018: Statistical-dynamical downscaling of the urban heat island in Hamburg, Germany. – Meteorol. Z. **27**, 89–109.

Hupfer, P., W. Kuttler, 2006: Witterung und Klima. – Teubner Verlag Wiesbaden, 554 pp.

Jacob, D., R. Podzun, 1997: Sensitivity studies with the regional climate model REMO. – Meteorol. Atmos. Phys. **63**, 119–129.

Liu, Y., H.V. Gupta, S. Sorooshian, L.A. Bastidas, 2004: Explore parameter sensitivities and model calibration in a locally coupled environment. – Bull. Amer. Meteor. Soc., publish online, 3365–3367.

Maronga, B., G. Gross, S. Raasch, S. Banzhaf, R. Forkel, W. Heldens, A. Matzarakis, M. Mauder, D. Pavlik, J. Pfafferott, S. Schubert, G. Seckmeyer, H. Sieker, K. Trusilova, 2019: Development of a new urban climate model based on the model PALM – Projectoverview, planned work and first achievements. – Meteorol, Z.

Marzban, C., X. Du, S. Sandgathe, J.D. Doyle, Y. Jin, N.C. Lederer, 2018: Sensitivity Analysis of the Spatial Structure of Forecasts in Mesoscale Models: Continuous Model Parameters. – Mon. Wea. Rev. **146**, 967–982.

Pelletier, J.D., J.P. Field, 2016: Predicting the roughness length of turbulent flows over landscapes with multi-scale microtopography. – Earth Surf. Dynam. **4**, 391–405.

Pielke, R., 2001: Mesoscale meteorological modelling. 2nd Ed. – Academic Press, Orlando, 676 pp.

Scherer, D., F. Ament, S. Emeis, U. Fehrenbach, B. Leitl, K. Scherber, Ch. Schneider, U. Vogt, 2019: Three-dimensional observation of atmospheric processes in three German cities. – Meteorol, Z. **28**, DOI: 10.1127/metz/2019/0911.

Sozzi, R., M. Favaron, 1998: Method for estimation of surface roughness and similarity function of wind speed vertical profile. – J. Appl. Meteor. **37**, 461–469.

Stull, R.B., 1988: An introduction to boundary layer meteorology. – Kluwer Academic, 666 pp.

Wippermann, F., 1973: The planetary boundary layer. – Ann. der Meteorologie **7**, Deutscher Wetterdienst Offenbach.

Yamada, T., 1982: A numerical model study of turbulent air flow in and above a forest canopy. – J. Meteor. Soc. Japan **60**, 439–454.

Ziemiański, M.Z., M.J. Kurowski, Z.P. Piotrowski, 2011: Toward very high horizontal resolution NWP over the alps: Influence of increasing model resolution on the flow pattern. – Acta Geophys. 59, 1205, DOI: 10.2478/s11600-011-0054-9.

Zhao, M., J.-C. Golaz, I.M. Held, V. Ramaswamy, S.-J. Lin, Y. Ming, P. Ginoux, B. Wyman, L.J. Donner, H. Guo, 2016: Uncertainty in Model Climate Sensitivity Traced to Representations of Cumulus Precipitation Microphysics. – J. Climate **29**, 543–560.